

Production and properties of electrically conductive polymer composites reinforced with cotton threads

Alexander P. Kondratov¹ | Anastasiya V. Lozitskaya¹ | Alex A. Volinsky² 

¹Department of Incognitive Technologies, Moscow Polytechnic University, Moscow, Russia

²Department of Mechanical Engineering, University of South Florida, Tampa, Florida, USA

Correspondence

Alex A. Volinsky, Department of Mechanical Engineering, University of South Florida, 4202 E. Fowler Ave. ENG030, Tampa, FL 33620, USA.
Email: volinsky@usf.edu

Abstract

The problem of strength loss in electrically conductive composites made with dispersed fillers in the polymer binder is solved by spraying an aerosol of graphite on a textile material with a 3D weave of threads, or on knitwear of fibers with various structure and chemical composition. The loose microstructure of cotton fibers and the developed surface of elastic filaments made of synthetic polymers retain colloidal graphite particles in a layered composite during cyclic deformation. The electrical conductivity of knitwear with graphite changes during stretching due to the reversible displacement of graphite particles, first during straightening and then during stretching of elastic threads. The 130 ± 5 strain sensitivity GF and $12,000 \pm 95 \text{ kPa}^{-1}$ stress sensitivity QF of the composites presented in this paper exceed the corresponding parameters of known electrically conductive composites. The combination of a significant change in electrical conductivity with the elasticity of the developed knitwear-based composite is important for the use in load cells, smart clothes, medical devices, and robotics.

KEYWORDS

conducting polymers, fibers, mechanical properties, sensors and actuators, textiles

1 | INTRODUCTION

Synthetic heterochain high-molecular compounds with intrinsic electrical conductivity are used to obtain electrically conductive polymer composites, along with carbon-chain and heterochain polymer compositions, filled with dispersions of inorganic substances with metallic-type conductivity.¹⁻³ The electrical conductivity of high-molecular compounds with intrinsic conductivity depends on the ambient temperature and their thermal manufacturing history. Electrical resistance of films and fibers made from such polymers can change by several orders of magnitude after heat treatment.¹ The effects of ambient temperature and the inevitable heat treatment of polymer compositions filled with dispersions of inorganic substances during the formation of products are

significantly less.⁴ However, the treatment of polymer compositions filled with dispersions of inorganic substances by ionizing radiation during the molding of products also changes the temperature dependence of electrical conductivity, affected by the irradiation dose.^{5,6}

In order to use electrically conductive polymer composites as strain sensors and gauges, it is necessary to reduce or eliminate their electrical conductivity dependence on temperature in the 10–100°C range. The possibility of manufacturing such compositions from graphite, polyethylene, and polypropylene with a low percolation threshold of less than 2% has been demonstrated.^{2,7} Various structures that emit or dissipate heat have been made from ductile polymer composites containing graphite, as well as sensors that register small bending strains, but cannot measure large and reversible strains. Elastic

composites consisting of piezoelectric polymer fibers and an elastomeric binder, polydimethylsiloxane, have been developed for the production of compression sensors.⁸ The use of fibers and filaments from synthetic and natural polymers to produce elastic composites and sensors for large and reversible strains is quite promising. The possibility of measuring electrical resistance of composites made from various fibrous materials with a coating containing three different commercially available carbon dispersions used for stencil printing of radio frequency identification (RFID) tag antennas has been demonstrated.⁹ The role of fibrous material structure in increasing the electrical conductivity of the composite has been established, although there were no significant differences between the electrical conductivity of fibrous materials with a layer of carbon dispersions of various allotropic forms. Fibrous composites based on knitwear have a looser structure and higher electrical resistance than composites based on twill weave fabrics. Intelligent textile systems with integrated fiber-based load cells are used to monitor human movement.^{10–12} Highly elastic fabrics for so-called smart clothes made of fibers with a conductive layer or from a mixture of polymer and metal filaments have been studied.^{13–19} The strain sensitivity of a fiber composite largely depends on the fabric structure and the number of conductive filaments. It has been shown experimentally that in polymer composites filled with dispersions of electrically conductive inorganic substances, the percolation path and the number of contacting filler particle chains decreased during tensile deformation due to the growth of microcracks in the material.²⁰ The electrical resistance of growing microcracks is much higher than the deformable piezoresistive materials. Cracks can open and close in various ways during bending, torsion, stretching, and compression.²¹ The electrical conductivity of fibers and filaments significantly depends on the predominant localization of electrically conductive particles, their number on the surface of the filaments or in the volume of fibers. The location of the electrically conductive chains on the surface or in the volume of the filaments determines the electrical properties of composites based on the environment (impurities, temperature, and humidity).²²

Therefore, the main problem of the electrically conductive polymer composites technology and their practical application as sensors is to overcome the contradiction between increasing electrical conductivity by placing more conductive filler on the surface and the need to protect the conductive component from mechanical destruction, along with the negative effects of the environment (humidity). This problem is solved by using a fibrous material with a volumetric interlacing of threads as a reinforcing base and fixing particles

of conductive filler (graphite) in the microporous structure of the fibers and between the threads. Protection against mechanical destruction of the filler's adhesion to the polymer and the negative influence of the environment is provided by duplication of the composite material, that is, by placing an electrically conductive layer between the two outer layers. In this study, a new elastic electrically conductive fiber composite is described, and the air temperature (10–70°C) and relative humidity (40%–100%) effects on its strain sensitivity in the range of its possible use as a cyclic deformation sensor placed on human clothing are studied.

This problem is solved here by using a fibrous material with a volumetric interlacing of threads as a reinforcing base and fixing particles of a conductive filler (colloidal graphite) with a high-molecular surfactant (polytetrafluoroethylene) in the microporous structure of fibers and between the threads. Maintaining sufficient adhesion of the filler to the polymer and protecting the composite from mechanical destruction during cyclic deformation is ensured by duplicating the composite material with the placement of an electrically conductive layer inside the double-layer web. The solution to the problem of combining graphite with polymer described in this paper allows to increase the sensors' sensitivity and reduce the hysteresis of the electrical signal during cyclic deformations compared with published samples of electrically conductive composites. In this study, the percolation mechanism is described for small (<15%) and large deformations of electrically conductive fiber composites. The effects of air temperature (10–70°C) and relative humidity (40%–100%) on the strain sensitivity GF and stress sensitivity QF are discussed.

2 | MATERIALS AND METHODS

Starting materials used in this research were industrially produced and meet international manufacturing standards for their production. Graphite suspension in 2-propanol with polytetrafluoroethylene was used to apply an electrically conductive layer on the cotton knitwear composites from an aerosol package. The suspension of colloidal graphite in propanol (CRC Industries, USA) was used with a 0.88 g/cm³ density, and 65 wt.% graphite concentration in the dry residue. The average size of graphite particles in suspension was 6.8 ± 0.7 μm. The knitwear had stockinette stitching. The composition of the fibers was 65% cotton, 25% polyester, and 10% polyurethane (Velikiye Luki Knitting Factory TRIVEL, Russia). The qualitative and quantitative compositions of the suspension ingredients were monitored using the FT-801 IR Fourier spectrophotometer and the differential

scanning calorimeter (DSC, 204 Phoenix, Netzsch, Germany). The ratio of graphite and polytetrafluoroethylene in the dry residue of the suspension was determined by thermogravimetry using TGA/DSC 3+ in Figure 1. After thermal degradation and removal of polymer decomposition products, the mass of the sample decreased by 30 wt.%. This change in mass corresponds to the proportion of organic components. The concentration of graphite in the dry residue was about 65 wt.%. The content of graphite suspension with polytetrafluoroethylene on knitwear was 21–28 wt.%.

Laboratory $10 \times 70 \text{ mm}^2$ samples of sensors were cut from a knitted fabric and dispersion of graphite with polytetrafluoroethylene was sprayed from an aerosol package on one side. The amount of graphite on the cotton threads' surface was controlled by the sample mass change after spraying the suspension and vacuum drying in the desiccator. The volume fraction of reinforcing knitted fabric in the composite did not exceed $83 \pm 0.5 \text{ wt.}\%$. Preparation of samples made from electrically conductive fibrous material included the following steps:

1. Conditioning of an industrial knitwear sample in a desiccator for 5 days at $22 \pm 1^\circ\text{C}$ and 30% relative humidity;

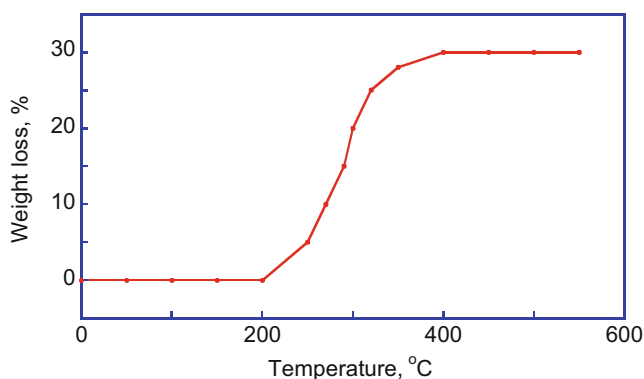


FIGURE 1 Thermogravimetric analysis of the solid phase of the suspension. [Color figure can be viewed at [wileyonlinelibrary.com](https://onlinelibrary.wiley.com)]

2. Spraying graphite dispersion with polytetrafluoroethylene in 2-propanol onto samples from an aerosol package from a 10 cm distance for 5 s, with a 0.07 m/s nozzle moving speed along the sample;
3. Cutting out ribbon samples with graphite-containing coating;
4. Manufacturing double-layer strain sensors by duplicating knitwear tapes with a graphite layer inside the double-layer material in Figure 2a;
5. Drying of coated samples at $20 \pm 1^\circ\text{C}$ and 30% relative humidity to a constant mass;
6. Measuring the mass of 10 identical samples using analytical scales with 0.0001 g resolution and calculating the average value;
7. Gluing copper foil electrodes with electrically conductive Keller contact glue on the surface of graphite-coated tapes in Figure 2b;
8. Conditioning samples in the desiccator before conducting mechanical tests and measuring electrical resistance at 10 and 70°C with 45% and 100% relative humidity.

A double-layer strain sensor was assembled from knitwear with an electrically conductive coating as follows. The segments of the tape of equal length were placed mirror-like and the segments were stacked in pairs on top of each other, that is, they duplicated the conductive layer inside the knitwear.²³ A flat electrode made of copper foil with wires was placed between the ends of the segments. The sample was placed in a universal tensile testing machine to obtain real-time load–displacement curves along with electrical measurements using a multimeter and a computer in Figure 3.²⁴

3 | RESULTS AND DISCUSSION

Fibrous composites consist of a knitted base, colloidal graphite, and thin layers of high-molecular compounds. Electrically conductive particles of colloidal graphite fill

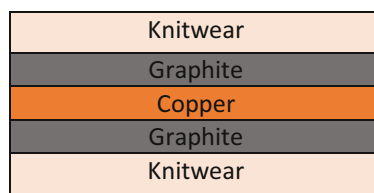
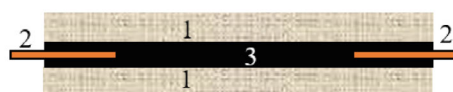


FIGURE 2 (a) Strain sensor cross-section schematics and (b) composite sample. Here, 1 are the knitwear layers, 2 are copper foil electrodes, and 3 is a graphite layer. [Color figure can be viewed at [wileyonlinelibrary.com](https://onlinelibrary.wiley.com)]



(a)



(b)

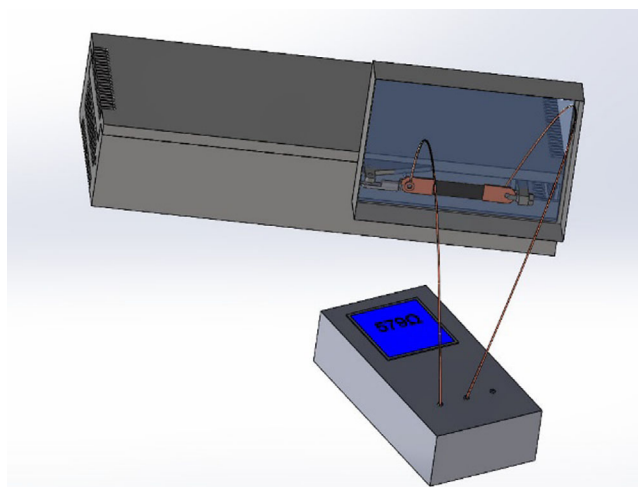


FIGURE 3 Schematics of universal tensile testing machine with mounted sample and multimeter for electrical characterization of the composite. [Color figure can be viewed at [wileyonlinelibrary.com](https://onlinelibrary.wiley.com)]

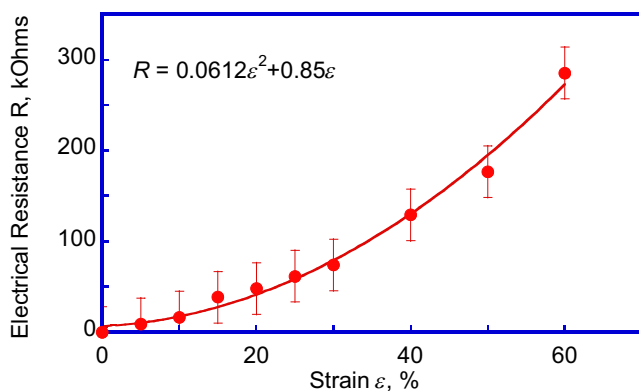


FIGURE 4 Composite electrical resistance changes when stretched. The error bars represent standard error. [Color figure can be viewed at [wileyonlinelibrary.com](https://onlinelibrary.wiley.com)]

the space between the fibers and are held on their surface by adhesion forces. The choice of fibers interlacing in the knitted base of strain gages and the tape cutting orientation relative to the direction of the fibers of the knitted base have been previously justified.²³

After treatment under different conditions, composites were tested by cyclic loading at a constant strain rate up to 50% strain. The electrical resistance of a 10 mm wide knitwear ribbon with a graphite layer increases by orders of magnitude when stretched to 60% in Figure 4.

Sensor samples made of electrically conductive composites were deformed with a 10 mm/min rate at $25 \pm 2^\circ\text{C}$ in the air and controlled relative humidity. Changes in the electrical resistance during stretching, normalized by the electrical resistance of undeformed sample ($\Delta R/R_0$) represent a sensor response to applied

strain in Figure 5. The strain sensitivity, also known as the calibration coefficient or a gauge factor GF is calculated as in¹⁵:

$$GF = \frac{(\Delta R/R_0)}{\Delta l/l_0}, \quad (1)$$

here, R_0 is the initial resistance of the strain sensor, ΔR is the relative change in resistance during deformation, l_0 is the initial sensor length, and Δl is the specimen elongation. The strain sensitivity GF is calculated from the slope of linear sections of the composite electrical resistance change with the applied strain.^{15,16}

To increase the accuracy of experimental data approximation by linear functions, measurements of the electrical resistance of knitwear at small 0%–15% tensile strains were repeated over 20 times, resulting in average values and confidence intervals in Figure 5. This strain range is of greatest practical importance when using composites as sensor materials for various devices, for example, patches and medical bandages used in monitoring facial expressions, breathing and heartbeat of a person in tight-fitted clothes.^{17,18} It can be seen that an increase in air humidity changes the strain sensitivity of composites by a factor of 2 during stretching and contraction. At the same time, the effects of humidity on the strain sensitivity of composites during stretching and contraction are different.

To determine the reason for the repeated change in the strain sensitivity of the composites under tension of more than 15%, an optical microscopy examination of the surface was performed with the construction of a 3D model of the relief and cross-section of the fabric along the threads of the knitwear in Figure 6a. According to the cross-section shape in Figure 6b, the warp threads are bent, so the knitted fabric is easily deformed to a certain elongation due to straightening in Figure 6d. It is reasonable to assume that when the threads are straightened, the continuity of the graphite layer on their surface is not affected significantly, resulting in continuous electrical resistance change in Figure 4.

Comparison of the profile curve length in Figure 6 with the dimensions of the knitwear sample confirms the assumptions that when stretched up to 15%–20%, the threads are straightened, which does not significantly affect the electrical resistance of the composite. When the knitwear is deformed by more than 15%–20%, the electrical resistance of the composite increases sharply due to an increase in the length and area of the outer surface of the threads, and cracking of the conductive layer on the surface.²¹

With elastic contraction of knitwear during unloading after stretching, contact between graphite particles is

FIGURE 5 Sensor output when stretched in the air with 45% (2) and 100% (3) relative humidity, and when contracted in the air after stretching at 45% (1) and 100% (4) relative humidity. The error bars represent standard deviation. [Color figure can be viewed at [wileyonlinelibrary.com](https://onlinelibrary.wiley.com/doi/10.1002/app.55410)]

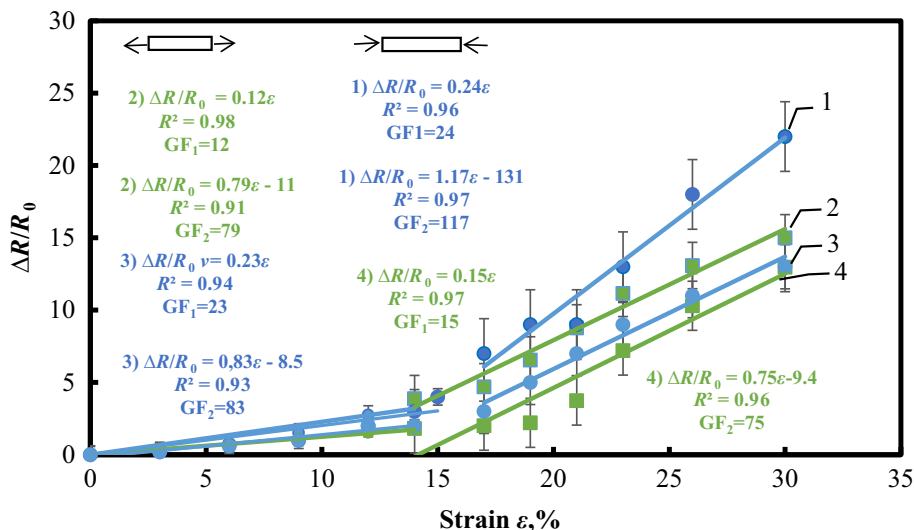
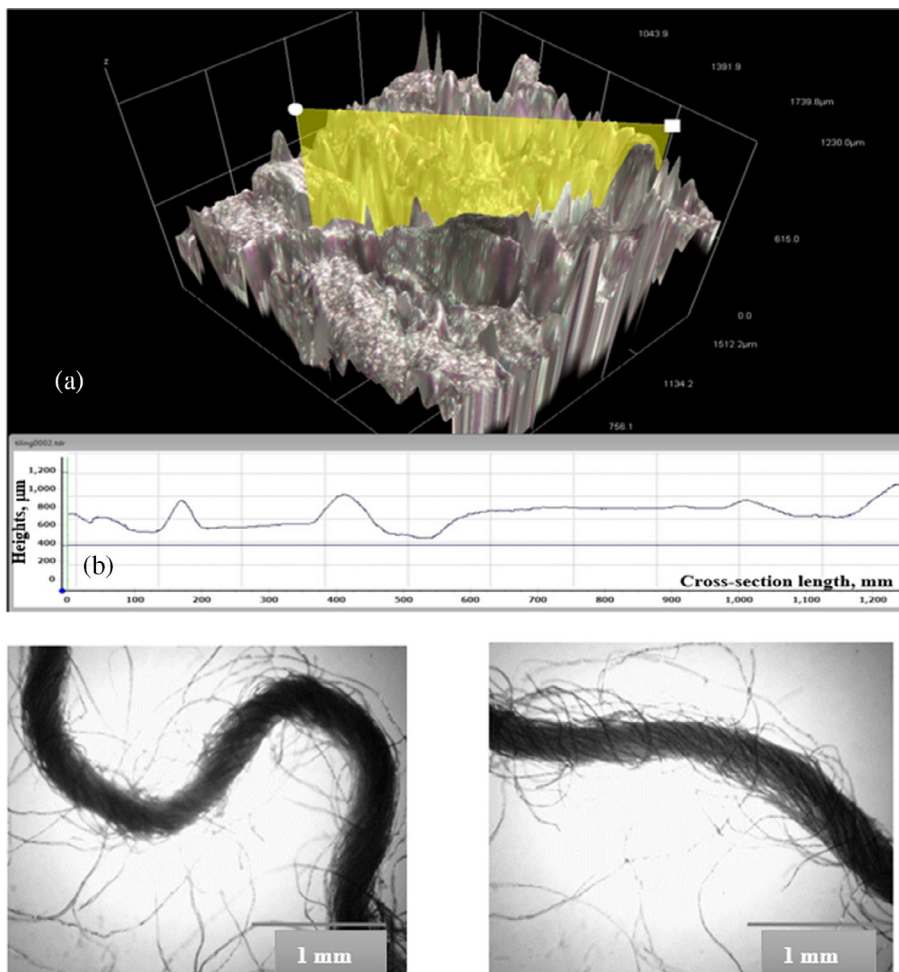


FIGURE 6 (a) 3D image of the sample surface and (b) the cross-section profile of knitwear along the fiber threads; c) photograph of a fiber extracted from knitwear, and (d) stretched fiber at 20% strain. [Color figure can be viewed at [wileyonlinelibrary.com](https://onlinelibrary.wiley.com/doi/10.1002/app.55410)]



restored and electrical conductivity increases. The strain sensitivity of a fibrous composite GF varies up to 130 for laboratory samples obtained under the patent,²³ and is not inferior to the published values for the composites with various electrically conductive fillers in Table 1.^{25–34} Table 1 lists the maximum GF values from the literature and obtained in this paper, which are higher.

For the practical application of composites in smart clothing, it is of interest to study the electrical response of strain sensors in the air temperature range, at which outerwear is usually used. To determine the effects of temperature on the electrical properties of fiber composites, the resistance of samples in hot and cold air was measured and the sensor output

TABLE 1 Strain sensitivity GF of the composites from various sources.

Composite matrix	Filler	Concentration, wt. %	Mixing and molding method	GF
Polyvinylchloride (PVC plastisol) ²⁵	Carbon black	1.5	Mixer	3.2–4.6
Thermoplastic elastomer (TPE) ²⁶ Термоэластопласт (TPE) ²⁶		50	Stirrer	20–80
Epoxy vinyl polyester ²⁷	Multi-walled carbon nanotubes (MWCNT)	0.3	Stirrer and ultrasonic mixer	2.6
Polycarbonate ²⁸		5	Injection molder	3.65–6.2
Bisphenol-F epoxy resin ²⁹		1	Planetary mixer	23
Polyethylene oxide ³⁰		0.9–2.5	Stirrer and ultrasonic mixer	3.7
Polymethyl methacrylate ³¹		1	Stirrer and ultrasonic mixer	15
Polyvinyl chloride (PVC) ²⁵		0.5–30	Stirrer	3.17
Copolymer ethylene terephthalate/ethylene vinyl acetate (PET/EVA) ³²	Graphene	-	Thermopressing	34
Polydimethylsiloxane (PDMS) ³³	ZnO nanowire	-	Mixing in solution	120
Polydimethylsiloxane (PDMS)/polystyrene ³⁵	Silver	36.7	Mixing in solution	17–78.6
Knitwear (cotton and polyester)/polytetrafluoroethylene (PTFE)	Colloidal graphite	20	Aerosol spraying	130 ± 5

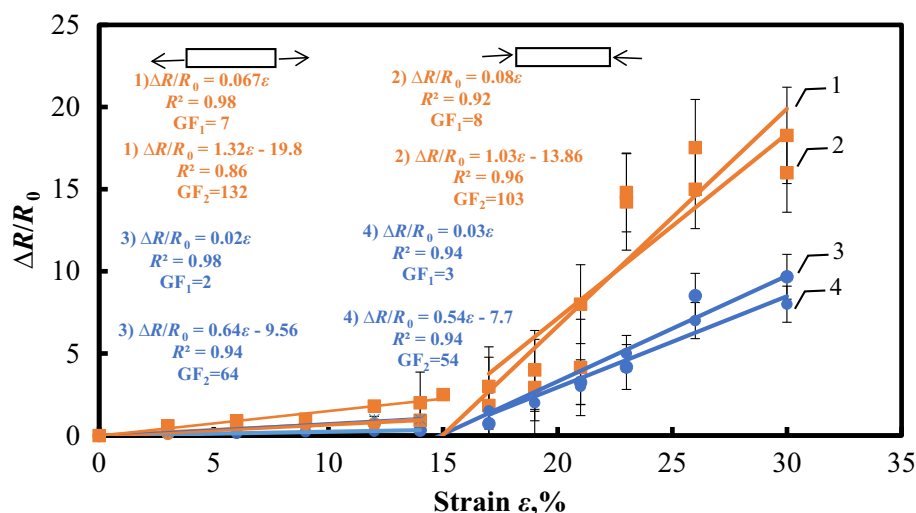


FIGURE 7 Sensor output in cold and hot air during stretching at 45% relative humidity: 70°C (1) and 10°C (3) and contraction after stretching at 70°C (2) and 10°C (4). The error bars represent standard deviation. [Color figure can be viewed at [wileyonlinelibrary.com](https://onlinelibrary.wiley.com/terms-and-conditions)]

was determined at 10 and 70°C at 45% relative humidity.

Figure 7 shows the change in the electrical resistance of fibrous composites at 70 and 10°C and 45% normal air humidity. At 70°C GF increases by 2–3 times during stretching and contraction after stretching. The strain sensitivity increase is especially noticeable with the air temperature increase and cyclic deformation of less than 15%, at which the composite threads are straightened.

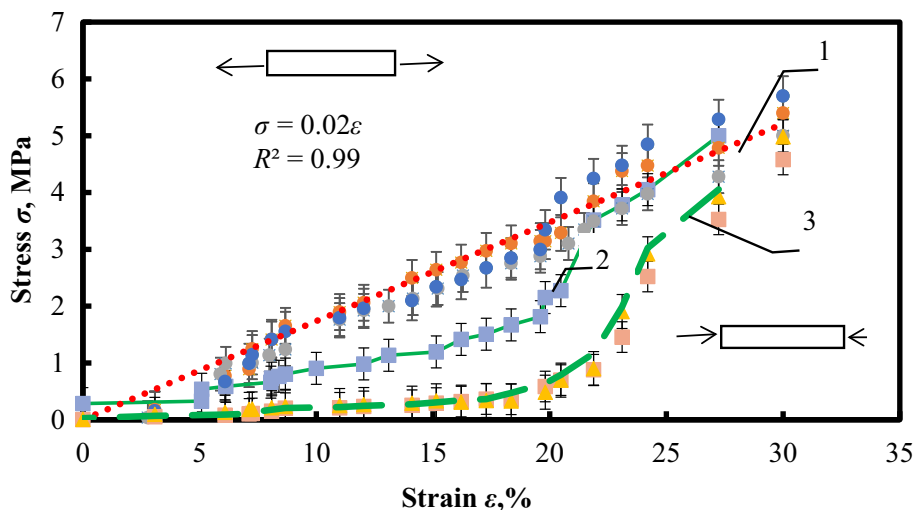
The resistance of conductors with metallic-type electrical conductivity increases when heated.³⁶ A similar temperature dependence of the electrical resistance in polymer composites with dispersed metals and graphite has been established.³⁷ Since the electrical properties of fibrous

composites are determined by the electrical conductivity of the graphite dispersion layer with polytetrafluoroethylene, it is legitimate to expect a decrease in electrical resistance with air temperature and its increase with cooling.

It can be concluded from the experimental results of changes in the electrical resistance of fibrous composites under cyclic deformations in Figure 7, and a comparative assessment of the calculated GF, that knitted fabrics coated with graphite dispersion both during stretching and contraction in hot and dry air have a significantly greater dependence on the strain magnitude than on humidity and air temperature.

To determine the true strain sensitivity, that is, the characteristics of the dependence of the electrical

FIGURE 8 Cyclic stress–strain curves of sensors during repeated stretching and contraction: 1, 2, 3, and 20 stretching-contraction cycles. The error bars represent standard deviation. [Color figure can be viewed at wileyonlinelibrary.com]



conductivity of the composite on mechanical stress,³⁸ it is necessary to know the mechanical properties of fibrous composites by measuring experimental values of the force arising in the material during stretching and elastic contraction.^{39–41} During mechanical tensile tests of the composite, it is possible to reliably measure the tension force of the tape with a known width, and the stress value can be characterized by a conditional load value, since it is impossible to determine the exact knitwear thickness under load. The functions of the conditional stress (load) from the relative elongation during cyclic deformation of composites during stretching and contraction are qualitatively different in Figure 8. This is the well-known Patrikeev–Mullins effect,⁴² which has significant features in the cyclic deformation of composites with reinforcing fibers.⁴³

During stretching, the stress in the composite increases monotonously and can be described by the linear equation with a constant conditional modulus of elasticity in Figure 8. When unloading, the stress change can be described by the two moduli, small in the 0%–15% strain range and large over 15% strain.

The tensile stress–strain curves show that the mechanical properties of the composites can be characterized by one value of the conditional modulus of elasticity of about 17 MPa. At the contraction stage, the conditional modulus of elasticity of the composite is 2 MPa when unloaded from less than 15% strain and 30 MPa when unloaded from larger strains. The stress sensitivity of the composite QF during tensile deformation is calculated as:

$$QF = \frac{\Delta R/R_0}{\Delta \sigma} [\text{Pa}^{-1}], \quad (2)$$

here, R_0 is the initial resistance of the sensors, ΔR is the change in resistance during deformation, and $\Delta \sigma$ is the increase in stress, respectively.

Table 2 summarizes the results of calculating the strain and stress sensitivity of knitwear-based composites at different temperatures and humidity.

Figure 9 shows the change in the electrical conductivity of a knitwear-based composite under cyclic tensile loading. The first deformation cycle has a significantly greater change in electrical conductivity up to 30% strain than subsequent cycles. This difference occurs both during stretching and during contraction. The second and further (up to 100 times) cyclic deformation of a composite based on graphite-coated knitwear does not affect its structure and properties. A stable state of the composite is achieved with reproducible and identical values of strain sensitivity GF_1 and GF_2 , and stress sensitivity QF_1 and QF_2 over the entire investigated strain range.

The test results, including the first cycle of reversible deformation of knitwear and 3 subsequent cycles of hysteresis are presented in Table 3. The hysteresis in Table 3 is calculated according to the Simpson formula¹⁹ with the calculation of the integral of the function of the change in electrical resistivity from deformation Equation (2):

$$\begin{aligned} h &= \int_a^b \left(\frac{\Delta R}{R} \right)_0 (\epsilon) d\epsilon \\ &\approx \frac{\Delta \epsilon}{3} \left[\left(\frac{\Delta R}{R} \right)_0 + 4 \left(\frac{\Delta R}{R} \right)_1 + 2 \left(\frac{\Delta R}{R} \right)_2 \right. \\ &\quad + 4 \left(\frac{\Delta R}{R} \right)_3 + \dots + 2 \left(\frac{\Delta R}{R} \right)_{n-2} + 4 \left(\frac{\Delta R}{R} \right)_{n-1} \\ &\quad \left. + \left(\frac{\Delta R}{R} \right)_n \right], \end{aligned} \quad (3)$$

here, ϵ is the strain, $\left(\frac{\Delta R}{R} \right)$ is the change in resistance, a and b are the limits of the change in resistance $\left(\frac{\Delta R}{R} \right)$ during deformation, n is the number of intervals of the electrical resistance dependence on strain, $\Delta \epsilon$ is the

Deformation conditions	Strain sensitivity GF		Stress sensitivity QF, κPa^{-1}	
	GF ₁	GF ₂	QF ₁	QF ₂
Tensile strain range, %				
Temperature, °C	0–15%	15–30%	0–15%	15–30%
10 ± 2°C	2 ± 0.5	64 ± 4	117 ± 45	3764 ± 73
70 ± 3°C	7 ± 1	130 ± 5	411 ± 62	7647 ± 81
Relative humidity, %				
45 ± 3%	23 ± 3	83 ± 5	1353 ± 63	4882 ± 72
100%	12 ± 2	79 ± 4	705 ± 63	4647 ± 77
Contraction strain range, %				
Temperature, °C	15–0%	30–15%	15–0%	30–15%
10 ± 1°C	3 ± 0.8	54 ± 4	1500 ± 68	1800 ± 67
70 ± 1°C	8 ± 1	103 ± 5	4000 ± 70	3433 ± 70
Relative humidity, %				
45 ± 3%	24 ± 3	117 ± 5	12,000 ± 95	3900 ± 78
100%	15 ± 2	75 ± 4	7500 ± 81	2500 ± 73

TABLE 2 Strain sensitivity GF and stress sensitivity QF of the sensors.

Note: Bold value emphasize the strain range.

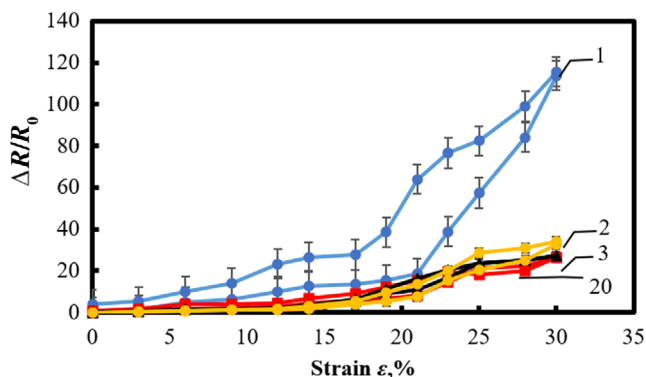


FIGURE 9 Sensor signal during cyclic deformation. Here, 1, 2, 3, and 20 are loading–unloading deformation cycles. The error bars represent standard deviation. [Color figure can be viewed at wileyonlinelibrary.com]

integration step along the strain axis ε , and ε_{\downarrow} is the strain direction (stretching or contraction).

Small hysteresis becomes especially important when composites are used as cyclic dynamic loading strain sensors, for example, in the manufacture of wearable electronics elements. Exceeding the hysteresis by more than 6% leads to the accumulation of plastic deformation and an irreversible decrease in the sensitivity of the composite to deformation and dynamic loading.

4 | CONCLUSIONS

1. A new elastic electrically conductive fiber composite has been obtained, and a method for its manufacture

TABLE 3 Hysteresis of electrical resistance during cyclic strain.

Deformation cycle number when measuring electrical resistance	Hysteresis h, %
1	50 ± 0.5
2	3.8 ± 0.3
3	3.4 ± 0.2
4	3.4 ± 0.2

Note: Bold values emphasize similar hysteresis values after the first cycle.

has been proposed. The possibility of using a layered composite as a cyclic strain sensor with a minimum (less than 4%) hysteresis of the electrical signal has been demonstrated.

- The method of manufacturing strain sensors includes applying an aerosol of a suspension of colloidal graphite with polytetrafluoroethylene to knitwear, duplicating knitwear tapes with a graphite layer inside a double-layer material, drying and a single pre-stretching to the maximum strain value measured by sensors in order to exclude signal hysteresis during cyclic deformation due to the Patrikeev–Mullins effect.
- The effects of air temperature and humidity (10 and 70°C temperature, 40% and 100% relative humidity) on the electrical resistance and strain sensitivity in the ranges of possible use of composites as cyclic deformation sensors placed on human clothing have been studied.
- The absolute values of the strain sensitivity GF and stress sensitivity QF of the sensors from the elongation

of a fiber composite sample in different ranges of tensile strain and elastic contraction are determined.

AUTHOR CONTRIBUTIONS

Alexander P. Kondratov: Conceptualization (lead); data curation (lead); formal analysis (lead); investigation (lead); methodology (lead); project administration (lead); resources (lead); supervision (equal); visualization (equal); writing – original draft (equal); writing – review and editing (equal). **Anastasiya V. Lozitskaya:** Conceptualization (equal); data curation (equal); formal analysis (equal); investigation (equal); methodology (equal); visualization (equal); writing – original draft (equal); writing – review and editing (equal). **Alex A. Volinsky:** Data curation (equal); formal analysis (equal); resources (equal); visualization (equal); writing – review and editing (lead).

DATA AVAILABILITY STATEMENT

The data that support the findings of this study are available from the corresponding author upon reasonable request.

ORCID

Alex A. Volinsky  <https://orcid.org/0000-0002-8520-6248>

REFERENCES

- [1] V. D. Noto, S. Lavina, G. A. Giffin, E. Negro, B. Scrosati, *Electrochim. Acta* **2011**, 57, 4.
- [2] X. S. Yi, G. Wu, D. Ma, *J. Appl. Polym. Sci.* **1998**, 67, 131.
- [3] D. Q. S. Ren, S. D. Zheng, S. L. Shilin Huang, Z. Y. Liu, M. Yang, *J. Appl. Polym. Sci.* **2013**, 129, 3382.
- [4] I. Chodak, M. Omastova, J. Pionteck, *J. Appl. Polym. Sci.* **1903**, 2001, 82.
- [5] P. Deng, P. Dong, J. Sun, *J. Appl. Polym. Sci.* **2002**, 85, 2742.
- [6] W. Xia, P. Zhang, *J. Appl. Polym. Sci.* **2021**, 138, 50295.
- [7] G. Yu, M. Q. Zhang, H. M. Zeng, *J. Appl. Polym. Sci.* **2015**, 70, 559.
- [8] N. W. Moon, *J. Appl. Polym. Sci.* **2020**, 137, 28.
- [9] A. V. Lozitskaya, A. P. Kondratov, *J. Phys. Conf. Ser.* **2022**, 2373, 092002.
- [10] T. Bashir, M. Ali, N. K. Persson, S. K. Ramamoorthy, M. Skrifvars, *Text. Res. J.* **2014**, 84, 323.
- [11] J. H. Lee, U. Khan, S. S. Kwak, R. Hinchet, S.-W. Kim, *Energy Environ. Sci.* **2018**, 11, 2057.
- [12] M. Monti, M. Natali, R. Petrucci, J. M. Kenny, L. Torre, *J. Appl. Polym. Sci.* **2011**, 122, 2829.
- [13] H. Zhang, X. M. Tao, T. X. Yu, *J. Sens. Actuat. A. Phys.* **2005**, 126, 803.
- [14] J. Zieba, *Fibres & Textiles in Eastern Europe* **2006**, 14, 43.
- [15] A. P. Kondratov, A. V. Lozitskaya, V. A. Baranov, E. P. Cherkasov, *IOP Conf. Series: Mat. Sci. Eng.* **2020**, 714, 012017.
- [16] Y. Huang, G. Tan, F. Gou, M. Li, S. Lee, S. Wu, *J. Soc. Inf. Disp.* **2019**, 27, 387.
- [17] N. Hu, Y. Karube, C. Yan, *Acta Mater.* **2008**, 56, 2929.
- [18] Y. Chen, F. Pan, S. Wang, B. Liu, J. Zhang, *Compos. Struct.* **2015**, 124, 292.
- [19] M. Mazaheri, J. Payandehpeyman, S. Jamasb, *Appl. Compos. Mater.* **2022**, 29, 695.
- [20] M. Knite, V. Teteris, A. Kiploka, *Sens. Actuators, A* **2004**, 110, 142.
- [21] H. Kawabe, Y. Natsume, Y. Higo, *J. Mat. Sci.* **1993**, 28, 3197.
- [22] F. Y. Zou, Y. H. Xu, H. Chen, L. Ye, *J. Adv. Mat. Res.* **2011**, 197-198, 396.
- [23] A. V. Lozitskaya, A. P. Kondratov, *R.F. Patent RU* (11). 2021, 2,762,026(13) 1.
- [24] S. V. Gunter, E. S. Marchenko, Y. F. Yasenchuk, G. A. Baigonakova, A. A. Volinsky, *J. Eng. Res. Exp.* **2021**, 3, 045055.
- [25] H. Yazdani, B. E. Smith, K. Hatami, *J. Appl. Polym. Sci.* **2016**, 133, 43665.
- [26] C. Mattmann, *Sensors* **2008**, 8, 3719.
- [27] J. J. Ku-Herrera, F. Aviles, *Carbon* **2012**, 50, 2592.
- [28] K. Parmar, M. Mahmoodi, C. Park, S. S. Park, *Smart Mater. Struct.* **2013**, 22, 075006.
- [29] N. Hu, Y. Karube, M. Arai, T. Watanabe, C. Yan, Y. Li, Y. Liu, H. Fukunaga, *Carbon* **2010**, 48, 680.
- [30] Y. Hu, T. Zhao, P. Zhu, Y. Zhang, X. Liang, R. Sun, C.-P. Wong, *Nano Res.* **2018**, 11, 1938.
- [31] G. T. Pham, Y. B. Park, Z. Liang, C. Zhang, B. Wang, *Composites, Part B* **2008**, 39, 209.
- [32] E. V. Boyko, I. A. Kostogrud, D. V. Smovzh, *J. Phys. Conf. Ser.* **2020**, 1677, 012125.
- [33] X. Xiao, L. Yuan, J. Zhong, T. Ding, Y. Liu, Z. Cai, Y. Rong, H. Han, J. Zhou, Z. L. Wang, *J. Adv. Mat.* **2011**, 23, 5440.
- [34] Z. Hu, Y. Xin, Q. Fu, *J. Polym. Res.* **2021**, 28, 134.
- [35] M. Park, H. Kim, J. P. Youngblood, *Nanotechnology* **2008**, 19, 055705.
- [36] R. A. Butera, D. H. Waldeck, *J. Chem. Educ.* **1997**, 74, 115.
- [37] A. Király, F. Ronkay, *J. Polym. Test.* **2015**, 43, 154.
- [38] J. Tang, Y. Wu, S. Ma, T. Yan, Z. Pan, *Science* **2022**, 25, 105162.
- [39] S. R. Larimi, H. R. Nejad, M. Oyatsi, A. O'Brien, M. Hoorfar, H. Najjaran, *J. Sens. Actuat. A. Phys.* **2018**, 271, 182.
- [40] A. Bose, X. Zhang, D. Maddipatla, *IEEE Sens. J.* **2020**, 20, 12652.
- [41] Z. C. Leseman, *J. Sci. Eng.* **2022**, 47, 1053.
- [42] A. P. Kondratov, A. V. Lozitskaya, V. N. Samokhin, A. A. Volinsky, *J. Polym. Res.* **2023**, 30, 36.
- [43] A. P. Kondratov, V. Konyukhov, S. Yamilinets, E. Marchenko, *Polymers* **2022**, 14, 5177.

How to cite this article: A. P. Kondratov, A. V. Lozitskaya, A. A. Volinsky, *J. Appl. Polym. Sci.* **2024**, 141(21), e55410. <https://doi.org/10.1002/app.55410>